Int. J. Electrochem. Sci., 16 **(2021)** Article Number: 21122, doi: 10.20964/2021.12.07

International Journal of
ELECTROCHEMICAL
SCIENCE
www.electrochemsci.org

Synthesis of Copolymers Based on Thiophene, Methoxythiophene, Propylenedioxythiophene and Quinoxaline Units and their Optical and Electrochemical Properties

Dehao Kong[1], *Shengyong Liu*[1,*], *Jinsheng Zhao*[2], *Yan Zhang*[2,*]

[1] School of Electric and Information Engineering, Guangxi University of Science and Technology, Liuzhou, 545006, China
[2] School of Chemistry and Chemical Engineering, Liaocheng University, Liaocheng, 252059, China
[*]E-mail: liusypp@163.com (S.Y. Liu); zhang_yan1219@126.com (Y. Zhang)

Received: 5 May 2021 / *Accepted:* 24 September 2021 / *Published:* 10 November 2021

Three D-A-type conjugated copolymers namely PTQET-1, PTQET-2 and PTQET-3 were designed employing quinoxaline units as the acceptor, thiophene, methoxythiophene and 3,4-propylenedioxythiophene (ProDOT) units as the donor. The three polymers had different feed ratio of the units and exhibited different electrochromic properties. They showed significant color changes during oxidation process with low optical band gaps as 1.51 eV for PTQET-1, 1.42 eV for PTQET-2, and 1.29 eV for PTQET-3. In particular, PTQET-2 and PTQET-3 displayed rare neutral black color. In the kinetic experiments, the three polymers presented high coloring efficiency and optical contrast in the near-infrared region, and especially PTQET-2 showed short switching time less than 1 s both in the near-infrared region and in the visible region. Besides, the polymers possessed favorable electrochromic stability and thermal stability. The new polymers reported in this paper provided a novel structural design for neutral black electrochromic materials, and they were worthy of attention and research.

Keywords: D-A type copolymers, thiophene derivatives, quinoxaline, electrochromism, neutral black

1. INTRODUCTION

The first example of conductive polymers can be traced back to the 1970s, scientists found that polyacetylene can be conductive after doping [1,2]. During these decades of research, a series of heterocyclic conjugated polymers similar to polyacetylene have been synthesized, including polythiophene [3], polypyrrole [4], polyaniline [5] and their derivatives. Conjugated polymers have many advantages of convenient preparation, low cost and light weight [6-8], which gives them widespread applications in light emitting diodes [9], organic solar cells [10] and electrochromic

materials [11]. Herein, a kind of novel conductive polymers with electrochromic feature is designed and researched.

Commonly, the conductive polymer with application potential consists of the π-conjugated backbone along with the solubilizing side chains [12,13]. It is generally acknowledged that the backbone determines the optoelectronic properties of the polymer and the side chain also plays crucial role in some aspects such as molecular weight, absorption, polymer solubility [14,15]. Therefore, the design of the conductive polymer structure should focus on both the conjugated backbone and the appropriate side chains. At present, constructing a conjugated backbone with donor-acceptor (D-A) type structure is an important method for preparing well-performing polymer [16-18]. By changing the types of acceptors and donors, numerous D-A type conductive polymers were developed and applied.

Quinoxaline is a promising building block as the acceptor unit structurally formed by the combination of a benzene ring and a pyrazine ring, and this structure not only improves the planarity of the corresponding polymer main chain, but also increases the length of the conjugated system, thereby making the π-π* dense packing stronger [12, 19-21]. In the quinoxaline rings, the two nitrogen atoms can enhance the electron-deficient capacity of the group, and moreover, the carbon atoms at 2,3-positions can be modified by different substituents to regulate the resulting polymer properties.

Thiophene and its derivatives have extensive application in the donor units because of their excellent electron transport ability, good redox stability, and ease of structural modification [22,23]. The advantages of thiophene-based conjugated polymers as organic photoelectric materials include excellent redox stability, highly polymerization, faster conversion speed, flexible mechanical performance [3,24]. Alkyl side chains are usually introduced into thiophene groups to enhance the solubility of the polymers and reduce its initial oxidation potential, but there is not much improvement in the electrochromic properties of the polymers. Therefore, some researchers synthesized a series of alkoxy-substituted thiophene derivatives (such as 3-methoxythiophene, 3-butoxythiophene, 3-butoxy-4-methylthiophene), and it was found that their corresponding polymers showed more stable doping process than the alkyl-substituted polymers [25-27]. In addition, the polymers based on 3,4-propylenedioxythiophene (ProDOT) and 3,4-ethylenedioxythiophene (EDOT) also possess high stability and good electrical conductivity [28-30].

In this paper, we selected 2,3-bis-(4-decyl-phenyl)-quinoxaline (M1) as the acceptor, thiophene (M2), 3,3-didecyl-3,4-dihydro-2H-thieno[3,4-b][1,4]dioxepine (M3) and 3-methoxythiophene (M4) as the donors to construct a novel kind of D-A type conjugated polymers. Three random copolymers were prepared using different feed molar ratio of M1/M2/M3/M4, which were named PTQET-1 (M1:M2:M3:M4 = 1:3:1:1), PTQET-2 (M1:M2:M3:M4 = 1:5:2:2) and PTQET-3 (M1:M2:M3:M4 = 1:4:1:2). Then a series of detailed analyses including electrochemistry, morphology, spectroelectrochemistry and switching kinetic were carried out, and the results indicated the three polymers, especially for PTQET-2, would be good candidates for electrochromic materials.

2. EXPERIMENTAL

All solvents and reagents employed in this study were used directly without further dispose. 2,5-Bis(trimethylstannanyl)thiophene was purchased from Derthon Optoelectronic Materials Science

Technology Co., Ltd. 3-Methoxythiophene was bought from Zhengzhou alpha chemical Co., Ltd. 5,8-Dibromo-2,3-bis-(4-decyl-phenyl)-quinoxaline and 6,8-dibromo-3,3-didecyl-3,4-dihydro-2H-thieno[3,4-b][1,4]dioxepine were synthesized in the light of the previous reports [30-32]. The schematic representation of the relevant syntheses was illustrated in Scheme 1. The specific synthesis steps of the compounds and polymers and the instruments used for the characterization were listed in the Supporting Information (SI).

PTQET-1: ^{1}H NMR (400 MHz, $CDCl_3$, δ ppm) 8.239-7.567 (m, 3H), 7.111-6.7223 (m, 2H), 4.174-3.948 (s, 1H), 3.948-3.704 (d, 2H), 1.904-1.011 (m, 58H), 1.002-0.522 (m, 9H) (see in SI, Figure S2a).

PTQET-2: ^{1}H NMR (400 MHz, $CDCl_3$, δ ppm) 7.946-7.557 (m, 3H), 7.020-6.674 (m, 7H), 4.342-4.251 (s, 1H), 4.116-3.915 (s, 1H), 3.915-3.704 (d, 4H), 1.626-0.911 (m, 229H), 0.911-0.546 (m, 71H) (see in SI, Figure S2b).

PTQET-3: ^{1}H NMR (400 MHz, $CDCl_3$, δ ppm) 7.986-7.615 (m, 8H), 6.976-6.631 (m, 7H), 4.942-4.764 (s, 1H), 4.227-3.939 (s, 5H), 3.939-3.713 (d, 7H), 1.921-1.002 (m, 221H), 1.002-0.599 (m, 34H) (see in SI, Figure S2c).

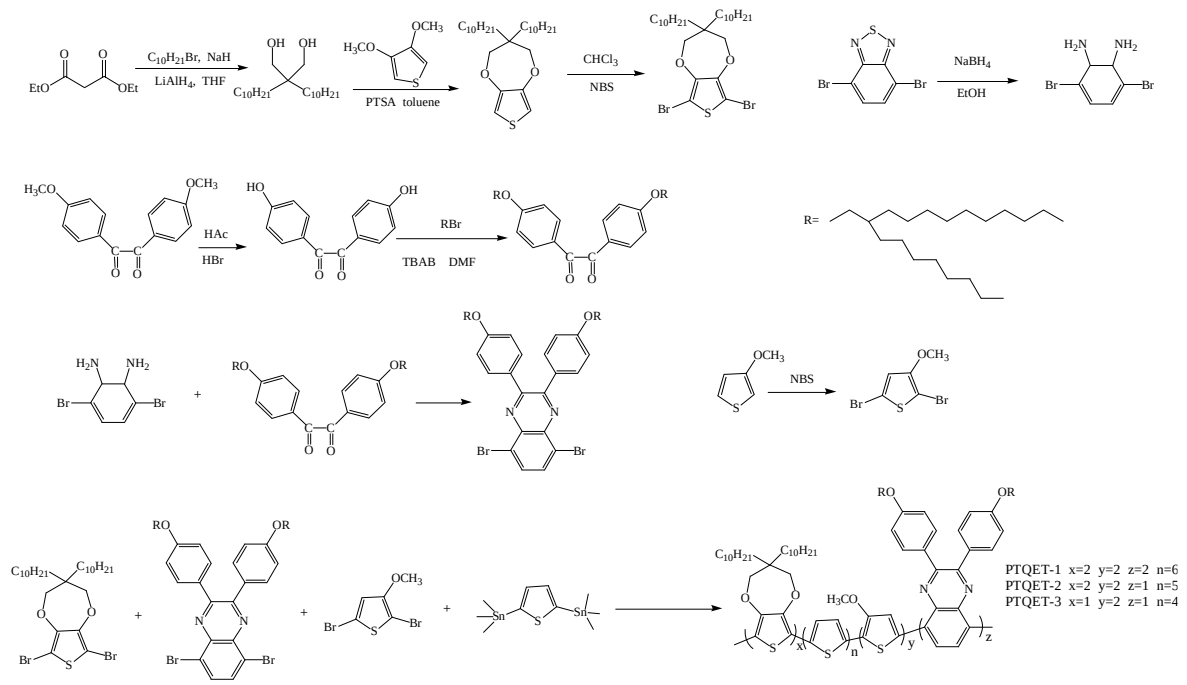

Scheme 1. Synthetic route of the compounds and polymers.

3. RESULT AND DISCUSSION

3.1. FT-IR spectra

FT-IR measurements aimed to verify the structures of the three polymers. As illustrated in Figure 1, the peak locations of the three polymers were almost identical as a result of their same monomer constitution, but the diverse molar ratio of the monomers caused the difference intensities of

the corresponding peaks. Taking PTQET-3 as an example, the absorption peaks from 720 cm^{-1} to 831 cm^{-1} corresponded to the C-H bending vibration in benzene, quinoxaline and thiophene rings. The weak absorption at 1093 cm^{-1} and the strong absorption at 1173 cm^{-1} in the fingerprint region were caused by the C-O-C stretching vibration [33]. The absorption peaks at 1464 cm^{-1}, 1511 cm^{-1} and 1605 cm^{-1} were derived from the stretching vibration of the aromatic ring framework in benzene, quinoxaline and thiophene rings. In addition, the absorption peaks at 2851 cm^{-1} and 2922 cm^{-1} were attributed to the C–H stretching vibration in the alkyl and alkoxy side chains. The appearance of these absorption peaks in the spectra indicated that all monomers were involved in the polymerization of the polymers and the target polymers were successfully synthesized.

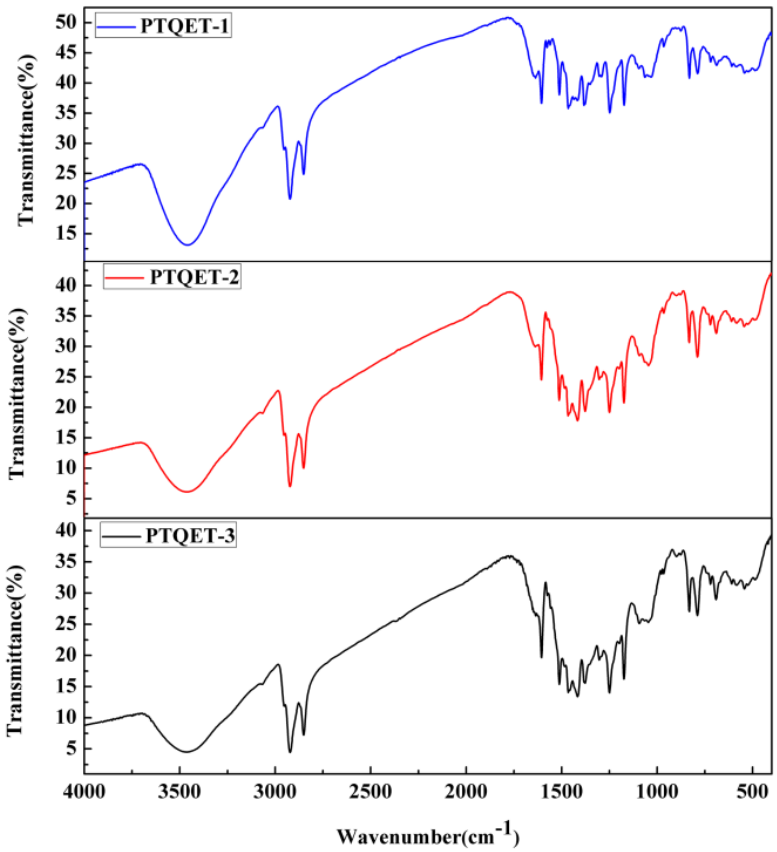

Figure 1. FT-IR spectra of PTQET-1 (a), PTQET-2 (b), and PTQET-3 (c).

3.2. Electrochemical properties

Each polymer was spray-coated on the ITO glass, and then cyclic voltammetry (CV) experiments were performed from -2.0 V to 2.0 V with 100 mV s^{-1} scan rate to explore their redox properties. As illustrated in Figure 2, the polymers started to be oxidized from the neutral state as the increase of potential. The tangent line of the positive-direction scanning can be used to obtain the initial oxidation potential (E_{onset}), and the specific results shown that the E_{onset} of three polymers were decreased gradually, corresponding to 0.93 V for PTQET-1, 0.84 V for PTQET-2 and 0.80 V for

PTQET-3, respectively. When the applied potential droped, the polymers gradually reduced and restored to the neutral state. All the three polymers showed obvious p-type doped redox peaks at positive potentials, and the corresponding values were 1.51 V / 1.06 V, 1.40 V / 0.86 V, 1.65 V / 0.45 V for PTQET-1, PTQET-2, and PTQET-3, respectively. During the negative-direction scanning, PTQET-1, PTQET-2, and PTQET-3 displayed reduction peaks at -1.53 V, -1.61 V, and -1.72 V respectively, but there was no obvious n-type oxidation peak, which might be caused by a very small amount of water and dissolved oxygen in the solution [34].

In addition, three D-A type copolymers (P1/P2/P3) derived from the literature, including different ratios of quinoxaline, ProDOT and benzene units, were used for comparison with PTQET-1, PTQET-2, and PTQET-3. And all three PTQET polymers had lower oxidation peak potentials and E_{onset} than P1/P2/P3 [33]. In contrast to another copolymer (P4) employing 7,8-bis(dodecyloxy)phenazine as acceptor and thiophene as donor, PTQET-1, PTQET-2, and PTQET-3 possessed lower E_{onset} [35]. Compare with the other three D-A type polymers (P5/P6/P7) based on different ratios of fluoro-substituted benzotriazidazole, thiophene and ProDOT units, the three PTQET polymers exhibited slightly higher oxidation peak potentials and E_{onset} [30].

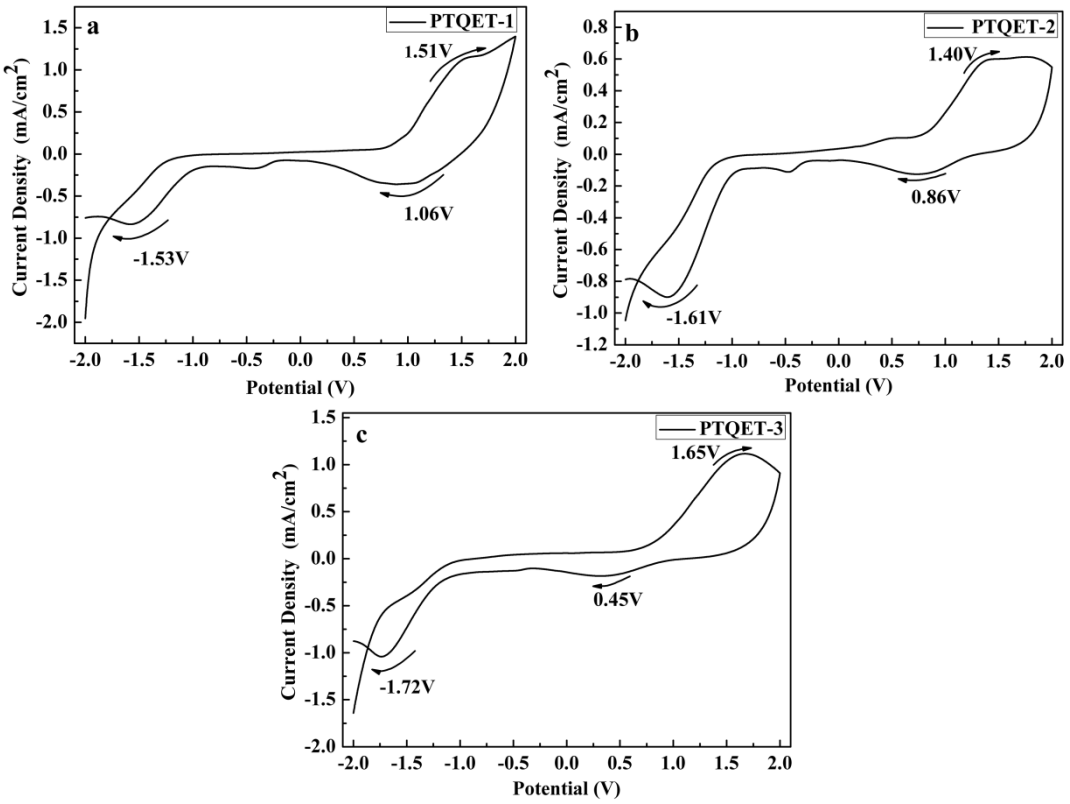

Figure 2. CV curves of PTQET-1 (a), PTQET-2 (b), and PTQET-3 (c). The experiments were executed in ACN solution using 0.2 M $TBAPF_6$ as supporting electrolyte in a three electrode cell system.

3.3. Morphology

Through the characterization of the morphology, the images of the film surface with 100 000 times magnification were shown in Figure 3, and it can be observed that the microscopic morphology of PTQET-1, PTQET-2, and PTQET-3 was similar because they were produce by the same monomers with different feed molar ratio. All three polymers have a relatively flat planar structure, which was related to their preparation process and was more conducive to the stability of oxidation-reduction process. Besides, many irregular cracks were present on the film surface, which was caused by the volatilization of solvent during the membrane formation [30]. Meanwhile, these streaks facilitate the doping of ions into and out of the polymers, thereby accelerating the redox switching and increasing their optical contrast.

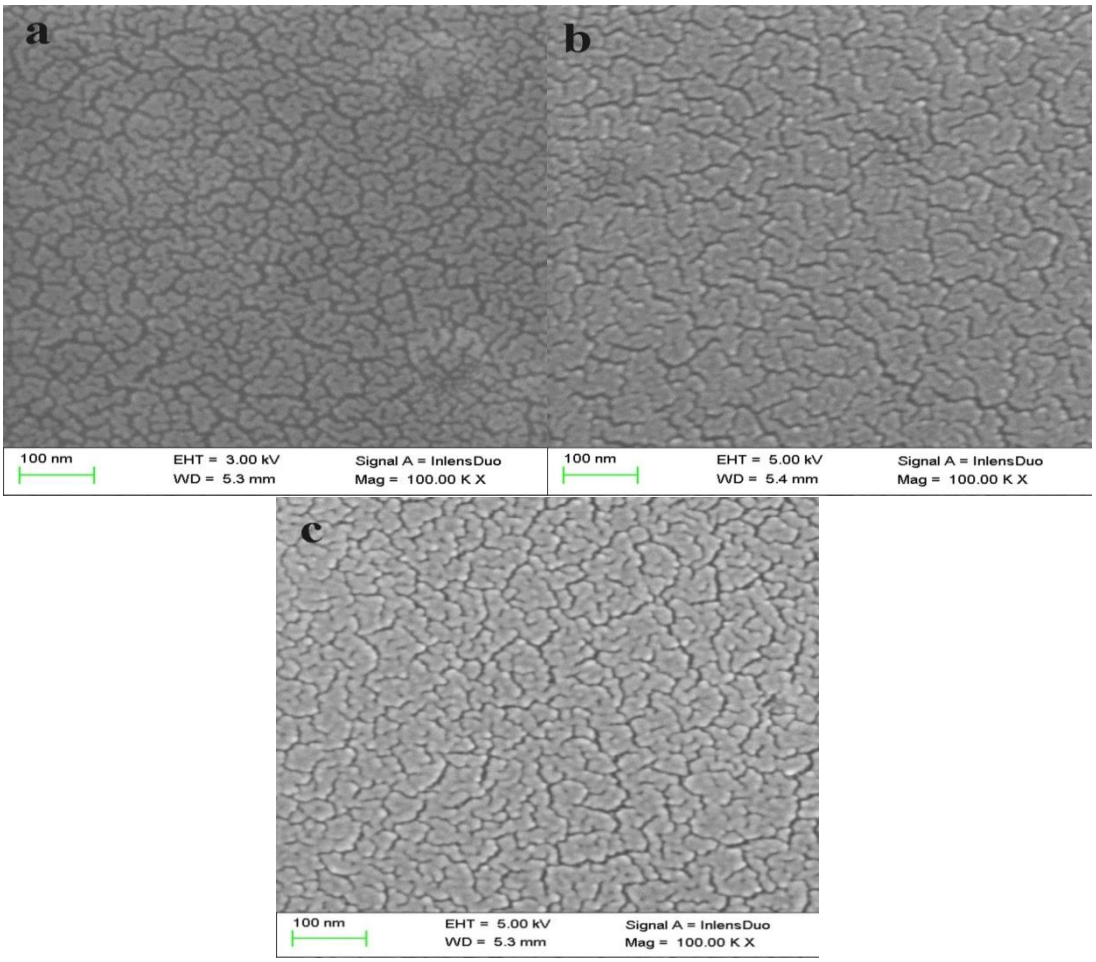

Figure 3. Morphology images of PTQET-1(a), PTQET-2(b), PTQET-3(c). The polymers were sprayed onto the ITO glasses.

3.4. Optical Properties

Each polymer was spray-coated on ITO glass and made into a solution (dichloromethane as solvent), respectively. Then their UV-Vis-NIR absorption spectra were detected, and the results were

illustrated in Figure 4. In terms of the polymer films (Figure 4a), the three polymers exhibited relatively broad absorption bands in the visible region. PTQET-2 and PTQET-3 had a wider coverage than PTQET-1 and their absorption covered the entire visible region, so PTQET-2 and PTQET-3 exhibited blackish to our eyes, while PTQET-1 exhibited grey in color. In terms of the polymer solutions, the absorption spectra were altered (Figure 4b), and they show distinct peaks in the visible region, which allowed the polymers to show different shades of purple in color. The maximum absorption wavelengths (λ_{max}) of PTQET-1 film and solution were 582 nm and 548 nm, the λ_{max} of PTQET-2 film and solution were 560 nm and 530 nm, and the λ_{max} of PTQET-3 film and solution were 608 nm and 524 nm. The λ_{max} of the polymer solid films took obvious redshifts compared to those of the polymer solutions, since the polymer films were more likely to form π-π* stacking, resulting in a stable conjugated structure [32].

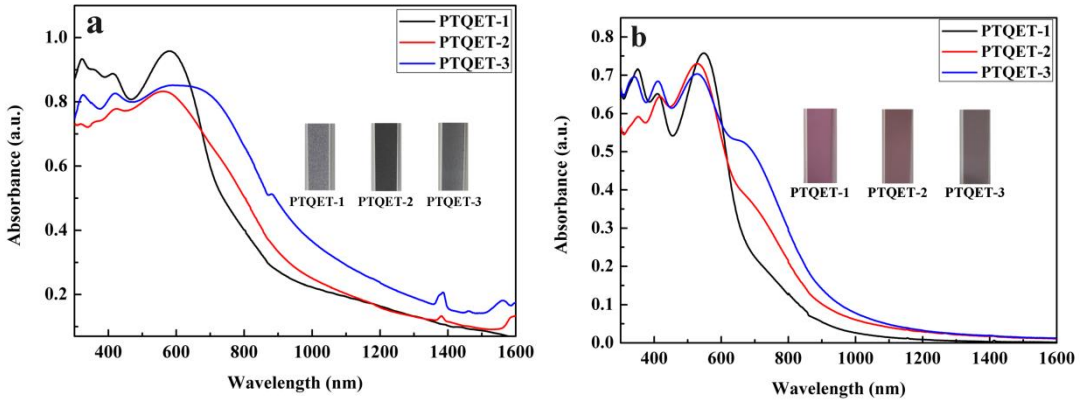

Figure 4. UV-Vis-NIR absorption spectra and photographs of polymer films (a) and polymer solutions (b).

3.5. Spectroelectrochemical Properties

Combined UV-Vis spectrophotometer and electrochemical workstation to conduct spectroelectrochemical experiments which was used to investigate the evolution of optical absorption as the polymers were oxidized step by step, and the results were shown in Figure 5.

In the neutral sate, the PTQET-1 film exhibited a maximum absorption peak located at 582 nm because of the π-π* transition (Figure 5a). With the increase of the applied potential, the forementioned absorption peak decreased by degrees, and meanwhile, two new absorption bands at about 830 nm and 1500 nm appeared and gradually enhanced as a result of the emergence of polaron and bipolaron. The decline of the absorption bands in the visible region faded the PTQET-1 film from gray (0 V) to floral white (1.1 V).

As suggested in Figure 5b, PTQET-2 demonstrated a wide absorption band covered the entire visible region in the neutral state, so it presented black color. As the potential increased, the above absorption band attenuated, while the polaron and bipolaron bands at 895 and 1475 nm in the near-infrared region gradually improved, making the color of PTQET-2 change from black to dark grey. For the PTQET-3 film, it demonstrated the similar trends of the absorption spectra with PTQET-2 as

suggested in Figure 5c, and its color converted from pale black to brown-gray in the oxidation process. In addition, PTQET-1, PTQET-2, and PTQET-3 exhibited isosbestic points at 685 nm, 674 nm, and 695 nm, respectively, suggesting that all the three polymers could realize the reversible conversion between the doped state and the dedoped state.

Some essential parameters of PTQET-1, PTQET-2, and PTQET-3 were summarized in Table 1. The λ_{onset} meant the onset wavelengths of the optical absorption spectra in the neutral state, and the $E_{g,op}$, E_{HOMO} and E_{LUMO} were determined using the following formulas $E_{g,op} = 1241/ \lambda_{onset}$, $E_{HOMO} = -e(E_{onset} + 4.4)$, $E_{LUMO} = E_{g,op} + E_{HOMO}$, respectively. The three polymers possessed relatively low optical band gap values, which was important for the application of the electrochromic materials.

Beside, several types of D-A type copolymers reported in the literatures mentioned above were also compared with the PTQET polymers. The first kind of copolymers P1/P2/P3 showed higher $E_{g,op}$ (2.06 eV/2.08 eV/2.05 eV) than the three PTQET polymers as well as different color changes from them [33]. The second copolymer P4 demonstrated reversible color change of blue-to-transmissive and had higher $E_{g,op}$ (1.57 eV) than the three PTQET polymers [35]. The third kind of copolymers P5/P6/P7 exhibited color changes from reddish brown or red to light gray, and they all possessed higher $E_{g,op}$ (1.77 eV/1.84 eV/1.86 eV) than PTQET-1, PTQET-2, and PTQET-3 [30].

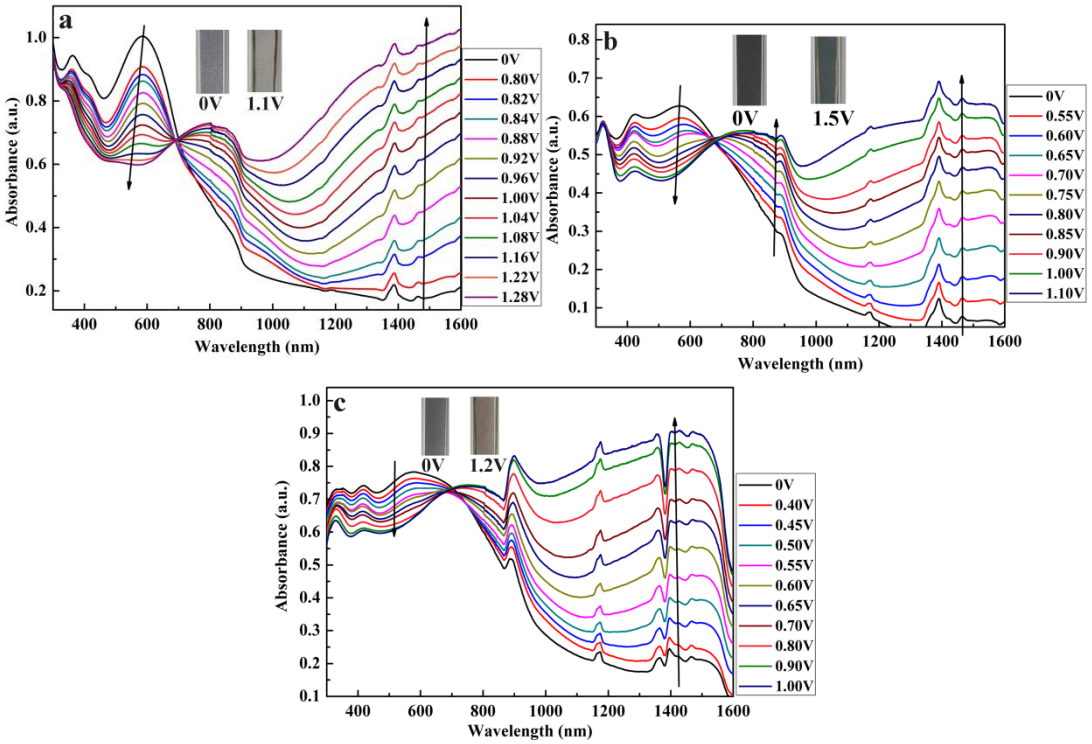

Figure 5. Spectroelectrochemical spectra of PTQET-1 (a), PTQET-2 (b), PTQET-3 (c) under different potentials. The polymers were spray-coateded on ITO glass, and the tests were executed in a 0.2 M $TBAPF_6$/ACN solution.

Table 1. Summary of essential parameters of PTQET-1, PTQET-2, and PTQET-3.

Polymer	λ_{onset}(film) nm	λ_{max}(solution) nm	λ_{max}(film) nm	E_{onset} V	$E_{g,op}$ eV	HOMO eV	LUMO eV
PTQET-1	820	548	582	0.93	1.51	-5.33	-3.82
PTQET-2	873	530	560	0.84	1.42	-5.24	-3.82
PTQET-3	964	524	608	0.80	1.29	-5.20	-3.91

3.6. Electrochromic Switching

To further characterize the electrochromic performance of PTQET-1, PTQET-2, and PTQET-3, the kinetic experiments were executed through the double potential step chronoamperometry technique. Figure 6 showed the optical contrast (ΔT%) during the transition of the polymers between the neutral state and the oxidized state for 300 s under the square wave potential with 4 s interval. And the corresponding kinetic parameters were listed in Table 2.

The ΔT% values were determined as 18.1% at 590 nm and 46.1% at 1500 nm for PTQET-1 (Figure 6a), as 14.5% at 570 nm and 41.4% at 1560 nm for PTQET-2 (Figure 6b), and as 9.0% at 575 nm and 36.8% at 1470 nm for PTQET-3 (Figure 6c). In contrast, the three polymers displayed relatively low ΔT% in the visible region, especially PTQET-3, while they demonstrated high ΔT% in the near-infrared region. Furthermore, the ΔT% maintained essentially unchanged within 300 s, indicating the good electrochromic stability of the three polymers.

The response time ($t_{95\%}$) was obtained by calculating the time spent for the polymer to achieve 95% maximum transmittance change in the oxidation process [36]. The $t_{95\%}$ of PTQET-1 were 1.45 s at 590 nm and 2.62 s at 1500 nm, the $t_{95\%}$ of PTQET-2 were 0.60 s at 570 nm and 0.71 s 1560 nm, and the $t_{95\%}$ of PTQET-3 were 2.37 s at 575 nm and 2.53 s 1470 nm (Table 2). It was found that PTQET-2 showed the shortest response time (less than 1 s) whether in the visible region or in the near-infrared region, suggesting that it could quickly complete the electrochromic conversion under the applied potential.

The coloring efficiency (CE) was calculated using the following equations: $CE = \Delta OD / \Delta Q$, $\Delta OD = \log (T_b / T_c)$, $\Delta Q = Q / A$. Therein T_b and T_c mean the transmittance in the neutral state and the oxidized state, respectively. Q means the total charge consumed in a cycle period. A refers to the active area of the ITO glass. As listed in Table 2, PTQET-1, PTQET-2, and PTQET-3 demonstrated high CE, particularly in the near-infrared region. By comparing the polymers, PTQET-2 possessed the highest CE both in the visible region and in the near-infrared region.

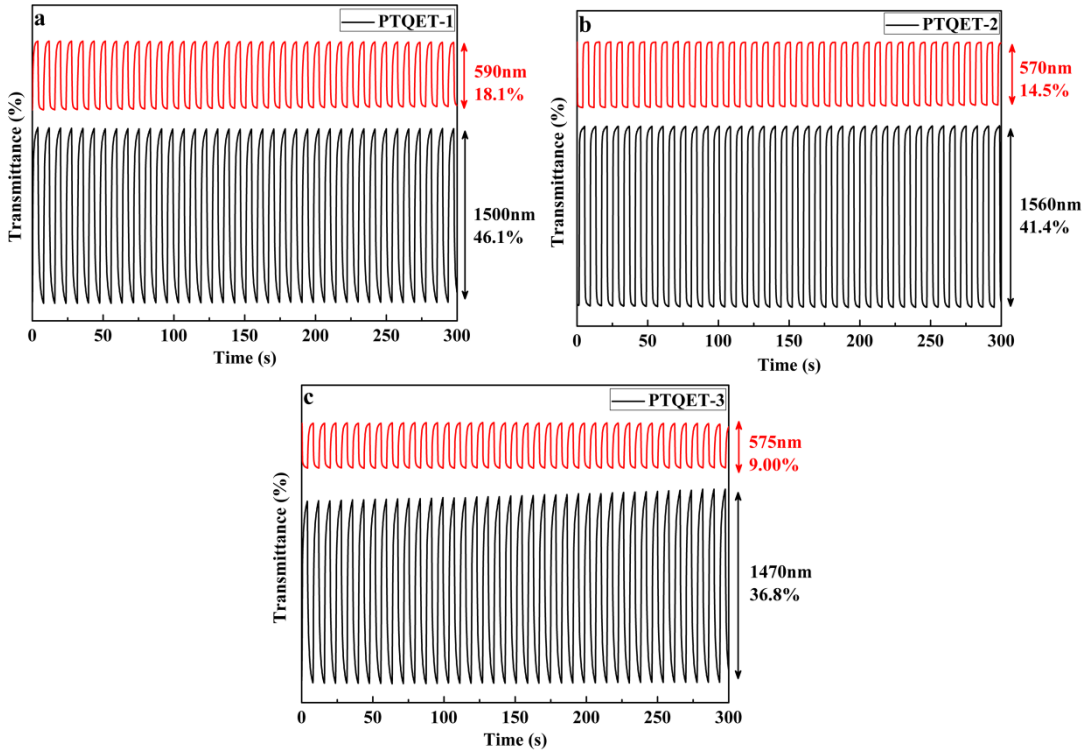

Figure 6. Electrochromic switching of PTQET-1 (a), PTQET-2 (b), and PTQET-3 (c) at different wavelengths. The tests were executed in a 0.2 M $TBAPF_6$/ACN solution under the square wave potential with the 4 s interval for 300 s.

Table 2. $\Delta T\%$,$t_{95\%}$ and CE of PTQET-1, PTQET-2, and PTQET-3.

Polymer	λ_{max} (nm)	$\Delta T\%$ (%)	$t_{95\%}$ (s)	CE ($cm^2 \cdot C^{-1}$)
PTQET-1	590	18.1	1.45	86.71
	1500	46.1	2.62	192.54
PTQET-2	570	14.5	0.60	114.91
	1560	41.4	0.71	305.06
PTQET-3	575	9.00	2.37	83.52
	1470	36.8	2.53	181.69

Moreover, the changes of $\Delta T\%$ were surveyed through varying the retention time of the kinetic experiments. For PTQET-1, the $\Delta T\%$ at 1500 nm declined from 52.6% (10 s), to 46.1% (4 s), to 40.0% (2 s), and to 33.6% (1 s), as well as those at 590 nm reduced from 20.1% (10 s), to 18.1% (4 s), to 15.2% (2 s), and to 12.3% (1 s), when the retention time gradually decreased (Figure 7). The $\Delta T\%$ of PTQET-1 at 1500 nm and 590 nm reduced by 19.0% and 7.8% respectively as the retention time dropped from 10 s to 1 s. The $\Delta T\%$ of PTQET-2 declined by 4.2% at 1560 nm and 0.6% at 570 nm (Figure S3), indicating that PTQET-2 could almost complete the transition between states within a retention time of

1 s, which was also consistent with its response time less than 1s as discussed above. In addition, the Δ*T*% of PTQET-3 reduced by 16.0% at 1470 nm and 3.06% at 575 nm (Figure S4). From the above comparison we can concluded that the appropriate increase in pulse duration is beneficial to improving the optical contrast of the polymers.

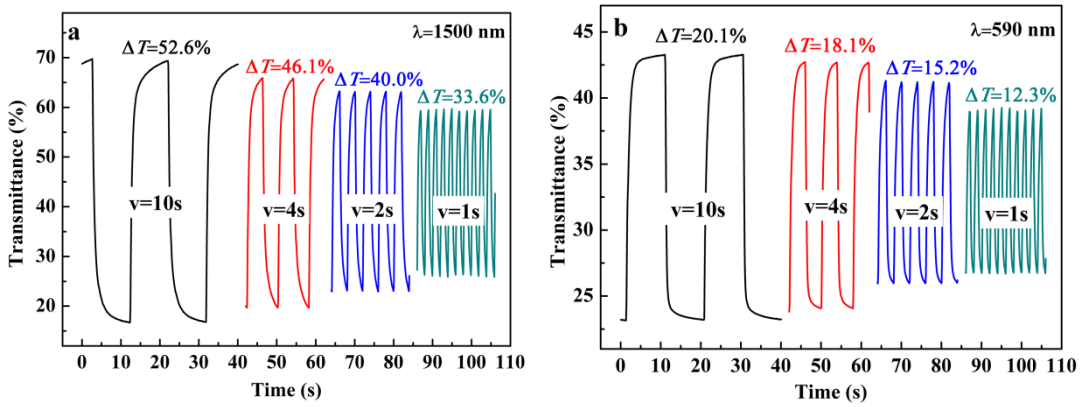

Figure 7. Electrochromic switching of PTQET-1 with intervals of 10, 4, 2 and 1 s at 1500 nm (a) and 590 nm (b). The tests were executed in a 0.2 M $TBAPF_6$/ACN solution under the square wave potential.

3.7. Colorimetry

To characterize the polymer color in detail, CIE 1976 *L**, *a**, *b** color space was used to test the brightness, color, and saturation. The L* and a*-b* curves of PTQET-1 under diverse potential conditions with different thickness (denoted by the maximum optical absorption) were recorded, and the results were shown in Figure 8, Figure S5 and Figure S6.

For PTQET-1, when the applied potential was 0 V, the *L** values gradually decreased from 75.89 to 61.34 and to 42.29 when the maximum optical absorption improved from 0.29 a.u. to 0.53 a.u. and to 0.95 a.u.. (Figure 8a). This indicated that the thinner polymer film allowed stronger light to pass through, which led to the increasing brightness and the L* value. For the PTQET-1 film with the same thickness, as the potential reached to 0.60 V, the color started changes and the corresponding *L** value became larger. As PTQET-1 continued to oxidation, the *L** value keep on increasing and then remained largely unchanged. When it was fully oxidized at 1.25 V, the *L** values corresponding to the three different thicknesses of the films were changed to 85.44, 75.66 and 57.09, respectively.

From the *a*-b** values of PTQET-1, the *a*/b** values of the PTQET-1 films with different thickness were 0.45/-2.63, 0.45/ -5.49 and 0.45/-5.97, respectively (Figure 8b). After completing the state transition, the *a*/b** values became to -1.36/3.58, -2.26/2.63, -1.36/3.58, respectively. In general, the *a*-b** values varied from the fourth quadrant to the second quadrant, and both the *a** and *b** values varied in a small range close to 0 throughout the oxidation. The color changed from gray to floral white with the oxidation of the PTQET-1 film, which was consistent with the results discussed earlier. From above discuss, we could concluded that the purpose of controlling the polymer color can be achieved by changing the film thickness and the applied potential.

In addition, the PTQET-2 and PTQET-3 films had the similar pattern in *L** and *a*-b** curves compared with PTQET-1, and the corresponding results were presented in Figures S5 and S6.

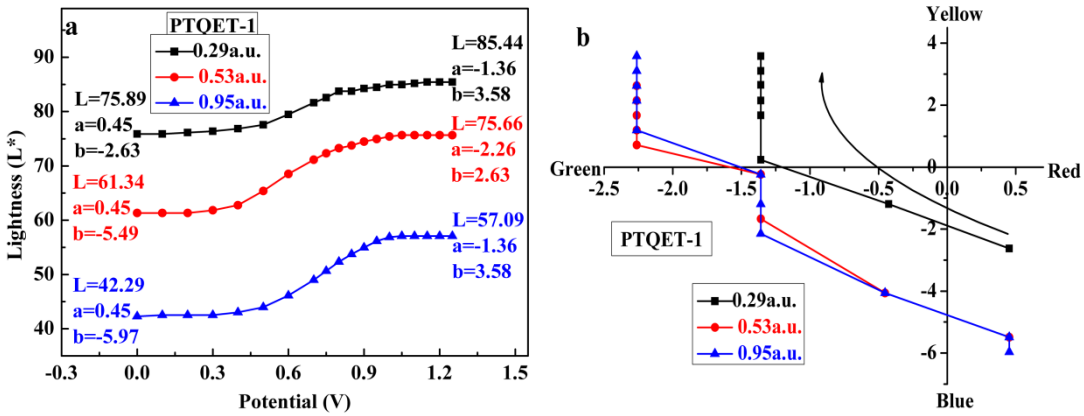

Figure 8. *L** and *a*-b** curves of PTQET-1 at different applied potentials.

3.8. Thermogravimetric Analysis

Thermal stability is also essential to the application of electrochromic polymers, which can be tested by TG experiments. The TG and differential thermal gravity (DTG) curves of PTQET-1, PTQET-2, PTQET-3 were displayed in Figure 9.

From the intersections of the tangent lines of the baseline and the degradation curve, we obtained the initial decomposition temperatures of the polymers [30], and the corresponding values were 398 °C, 387 °C and 366 °C, respectively, which preliminary showed that PTQET-1 had the best thermal stability. Then as the temperature increased, the molecular structures of the polymers were destroyed, and the polymer began to decompose rapidly. The temperatures at the maximum decomposition rate can be given by the DTG curve, and the specific values were 446 °C for PTQET-1, 444 °C for PTQET-2, and 444 °C for PTQET-3. Besides, from the TG curves we could see that when the temperature rose to 780°C, the remaining mass percentages of PTQET-1, PTQET-2, PTQET-3 were 20.7%, 11.5%, and 46.7%, respectively. According to the above data, it was found that the three polymers were able to withstand high temperatures, and in particular, the high initial decomposition temperature of PTQET-1 made it very suitable for high temperature resistant devices and other applications.

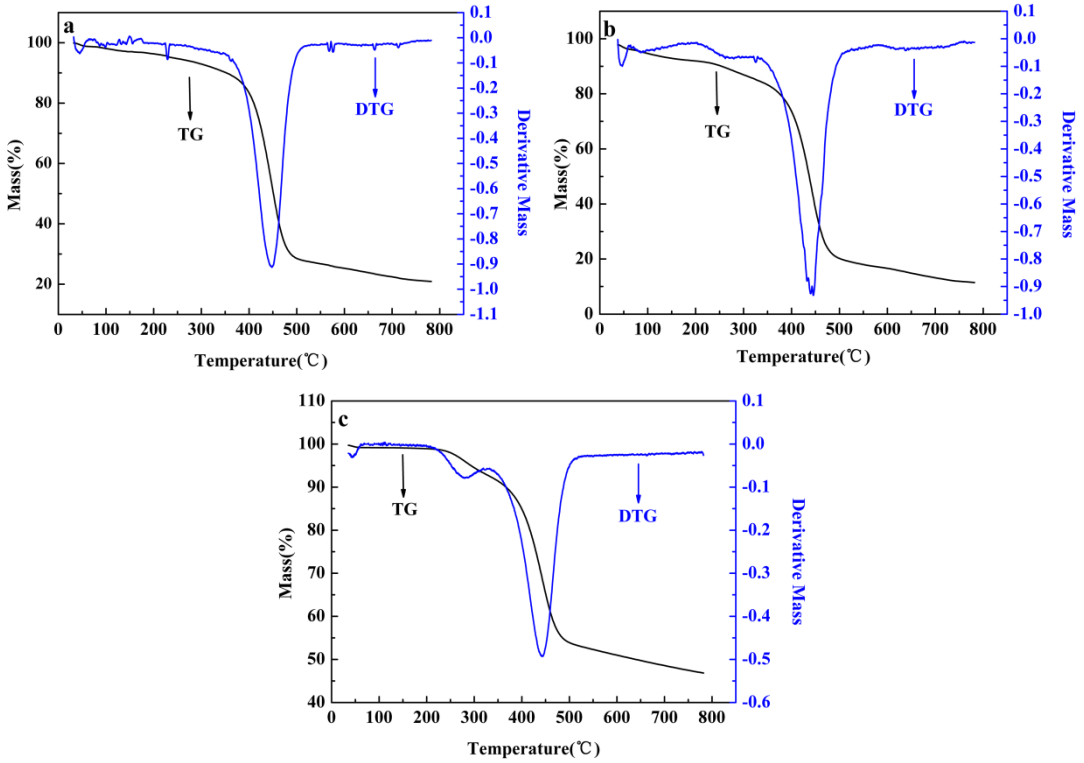

Figure 9. TG and DTG curves of PTQET-1 (a), PTQET-2 (b), and PTQET-3 (c). The tests were executed in nitrogen atmosphere with 10 ºC/min heating rate.

4. CONCLUSIONS

In this paper, we successfully synthesized three D-A type conjugated polymers named PTQET-1, PTQET-2 and PTQET-3 with different feed ratio of donor and acceptor units. All the polymers showed obvious redox peaks under the positive potential scanning in the CV tests. They all presented distinct color changes during oxidation, i.e., PTQET-1 was from gray to floral white, PTQET-2 was from black to dark grey, and PTQET-3 was from pale black to brown-gray. The three polymers had relatively low optical band gaps of 1.51 eV, 1.42 eV, and 1.29 eV for PTQET-1, PTQET-2 and PTQET-3, respectively. In addition, the three polymers demonstrated high optical contrast and coloring efficiency in the near-infrared region. In contrast with PTQET-1 and PTQET-3, PTQET-2 had the shortest response time and the highest coloring efficiency both in the visible and in the near-infrared region, and it also had the least loss of optical contrast with the reducing of the retention time. Moreover, the polymers all illustrated satisfactory thermal stability. These positive results indicated that the three novel polymers were promising candidates for electrochromic materials.

ACKNOWLEDGEMENTS
The work was financially supported by the Natural Science Foundation of Shandong Province (ZR2019MEM031).

SUPPORTING INFORMATION

Synthesis of 2,5-dibromo-3-methoxythiophene

5 g (43.86 mmol) 3-Methoxythiophene was dissolved in 300 mL mixed solution of methylene chloride and acetic acid (1:1, V/V), and then 19.49 g (109.50 mmol) N-bromosuccinimide (NBS) was added under stirring (considering the large number, NBS was added in four times). The reaction lasted for 24h at room temperature. After completion of the reaction, the resulting mixture was extracted three times using chloroform and deionized water. The organic layer was dried with magnesium sulfate and distilled under vacuum. Then the obtained crude product was purified through silica gel column chromatography to give a purple-black liquid (Yield, 90%). ^{1}H NMR ($CDCl_3$, 400 MHz, ppm): δ = 6.79 (s, 1H), 3.81(s, 3H). ^{13}C NMR ($CDCl_3$, 101 MHz, ppm): δ = 154.03, 120.09, 114.56, 91.84, 52.64 (see in SI, Figure S1).

Syntheses of PTQET-1, PTQET-2 and PTQET-3

The three polymers were prepared through Stille coupling reaction with different feed ratio.

For PTQET-1, 252.1 mg (0.244 mmol) 5,8-dibromo-2,3-bis-(4-decyl-phenyl)-quinoxaline, 300 mg (0.732 mmol) 2,5-bis(trimethylstannanyl)thiophene, 145.5 mg (0.244 mmol) 6,8-dibromo-3,3-didecyl-3,4-dihydro-2H-thieno[3,4-b][1,4]dioxepine, 66.4 mg (0.244 mmol) 2,5-dibromo-3-methoxythiophene, and 28.64 mg (0.041 mmol) bis-(triphenylphosphine) dichloropalladium ($Pd(PPh_3)_2Cl_2$) were added to 50 mL toluene. Then the mixture was refluxed at 105 ºC for 48 h under argon atmosphere. After the reaction was completed, toluene was removed through vacuum distillation to gain the crude product. Then the solid was extracted in a Soxhlet extractor using methanol and acetone respectively until the solution became colorless. The resulting PTQET-1 was dark grey solid.

For PTQET-2, the amounts of monomers were 151.3 mg (0.146 mmol) 5,8-dibromo-2,3-bis-(4-decyl-phenyl)-quinoxaline, 300 mg (0.732 mmol) 2,5-bis(trimethylstannanyl)thiophene, 174.2 mg (0.293 mmol) 6,8-dibromo-3,3-didecyl-3,4-dihydro-2H-thieno[3,4-b][1,4]dioxepine, 79.7 mg (0.293 mmol) 2,5-dibromo-3-methoxythiophene and 31.4 mg (0.045 mmol) $Pd(PPh_3)_2Cl_2$. The purified PTQET-2 was pale black solid.

For PTQET-3, the amounts of monomers were 189.2 mg (0.183 mmol) 5,8-dibromo-2,3-bis-(4-decyl-phenyl)-quinoxaline, 300 mg (0.732 mmol) 2,5-bis(trimethylstannanyl)thiophene, 109 mg (0.183 mmol) 6,8-dibromo-3,3-didecyl-3,4-dihydro-2H-thieno[3,4-b][1,4]dioxepine, 100 mg (0.366 mmol) 2,5-dibromo-3-methoxythiophene, and 26.81 mg (0.038 mmol) $Pd(PPh_3)_2Cl_2$. The purified PTQET-3 was dark gray solid.

Characterizations

The ^{1}H NMR and ^{13}C NMR spectra were measured by a Varian AMX 400 spectrometer with tetramethylsilane as the internal reference. The fourier transform infrared (FT-IR) spectra were measured by a Nicolet 6700 FTIR spectrometer. Microscopic morphology was obtained through a

Hitachi SU-70 thermionic field emission scanning electron microscope (SEM). Cyclic voltammetry experiments were executed on a CHI760 electrochemical workstation and the UV-Vis-NIR spectra were obtained by a Varian Cary 5000 spectrophotometer. The polymer films were spray-coated onto the ITO glass (active area of 0.9 cm × 3.0 cm). The electrolyte solution used in all experiments was prepared by dissolving 0.2 M tetrabutyl-ammonium hexafluorophosphate ($TBAPF_6$) in acetonitrile (ACN). The thermal gravimetric (TG) analysis was performed by a Netzsch STA449C TG/DSC simultaneous thermal analyzer.

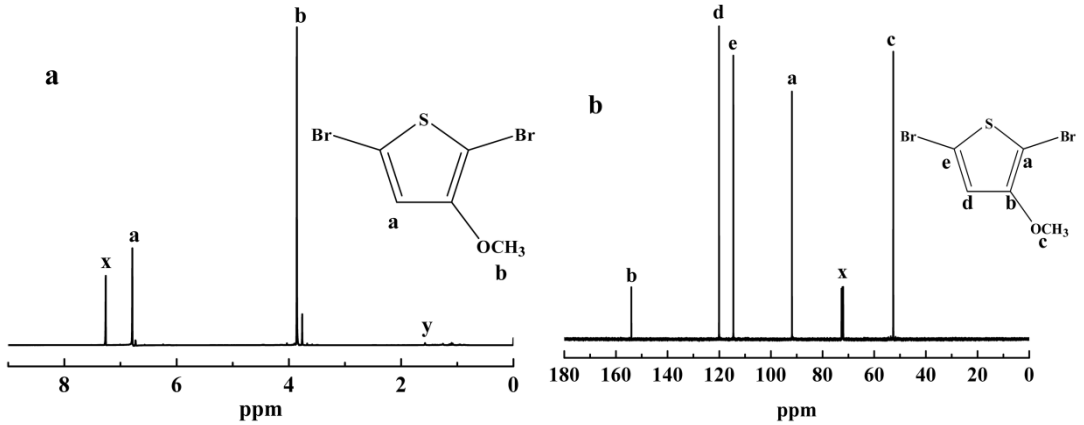

Figure S1. (a) ^{1}H NMR spectrum of 2,5-dibromo-3-methoxythiophene, $CDCl_3$ solvent peak and water peak were marked by 'x', 'y' respectively, (b) ^{13}C NMR spectrum of 2,5-dibromo-3-methoxythiophene, $CHCl_3$ solvent peak was marked by 'x'.

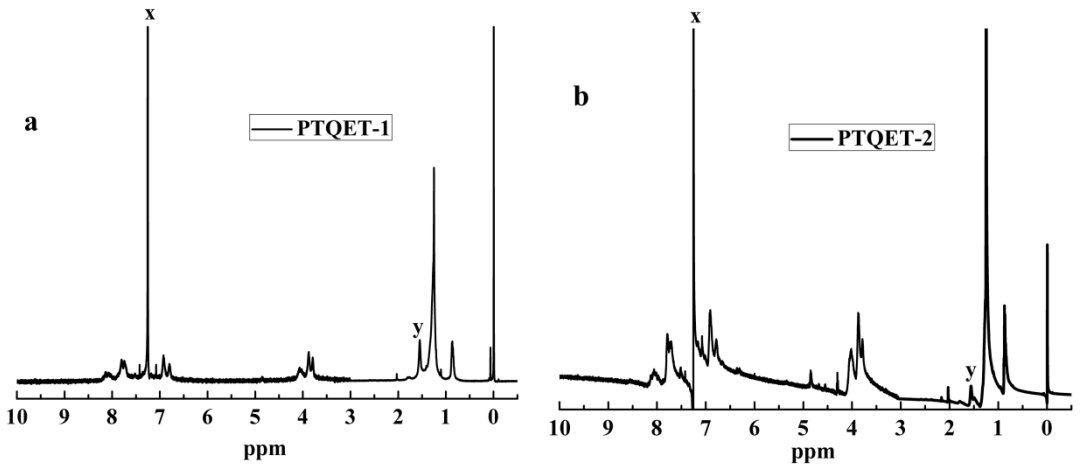

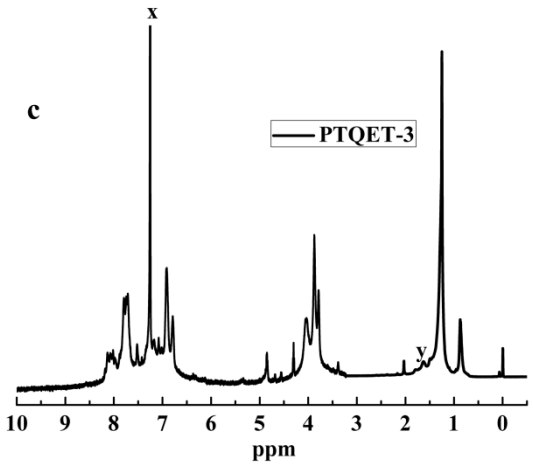

Figure S2. ^{1}H NMR spectra of PTQET-1 (a), PTQET-2 (b), and PTQET-3 (c), $CDCl_3$ solvent peaks and water peaks were marked by 'x', 'y' respectively.

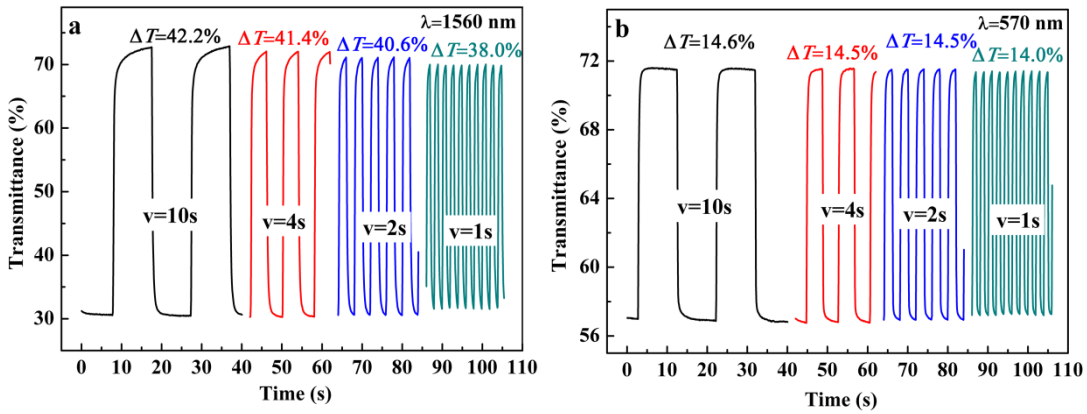

Figure S3. Electrochromic switching of PTQET-2 with intervals of 10, 4, 2 and 1 s at 1560 nm (a) and 570 nm (b). The tests were executed in a 0.2 M $TBAPF_6$/ACN solution under the square wave potential.

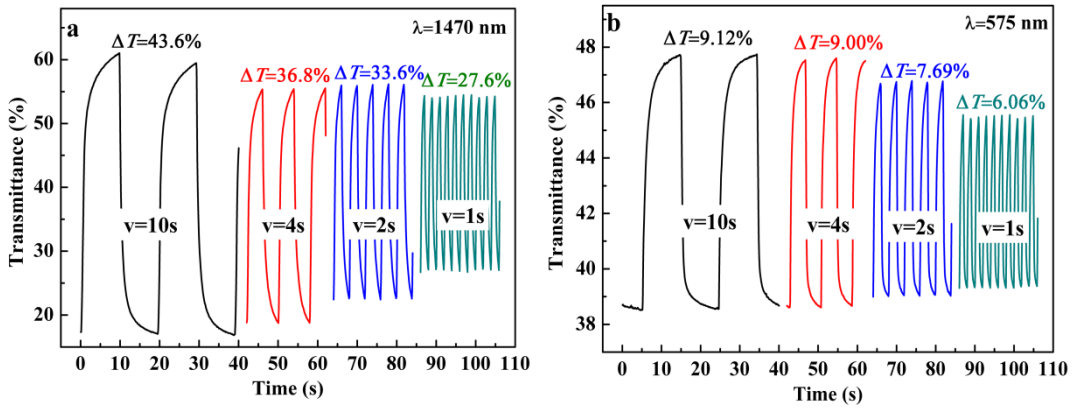

Figure S4. Electrochromic switching of PTQET-3 with intervals of 10, 4, 2 and 1 s at 1470 nm (a) and 575 nm (b). The tests were executed in a 0.2 M $TBAPF_6$/ACN solution under the square wave potential.

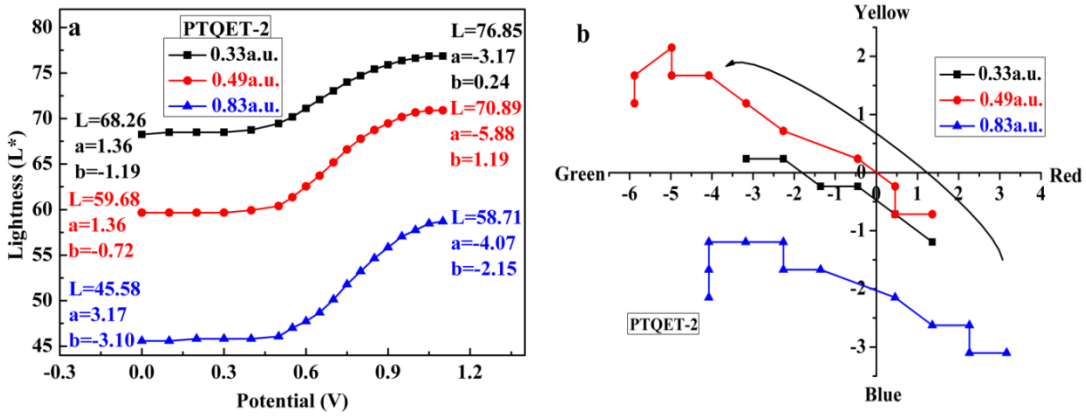

Figure S5. *L** and *a*-b** curves of PTQET-2 at different applied potentials.

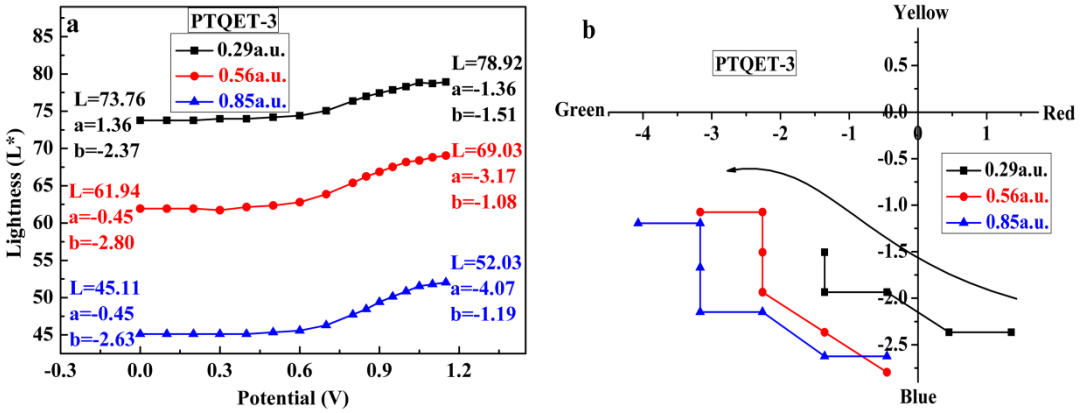

Figure S6. *L** and *a*-b** curves of PTQET-3 at different applied potentials.

References

1. M.Audenaert, G.Gusman and R.Deltour, *Phys. Rev. B.,* 24 (1981) 7380-7382.
2. C. K.Chiang, S.C. Gau, C.R. Fincher, Y.W. Park, A.G. MacDiarmid and A.J. Heeger, *Appl. Phys. Lett.,* 33 (1978) 18-20.
3. Z.D. Seibers, T.P. Le, Y. Lee, E.D. Gomez and S.M. Kilbey, *Acs Appl Mater Inter.,* 10 (2018) 2752-2761.
4. J. Lee, H. Jeong, R.L.Lavall, A. Busnaina,Y. Kim, Y.J. Jung and H. Lee, *ACS Appl. Mater. Inter.,* 9 (2017) 33203-33211.
5. F.W. Liu, S.J. Luo, D. Liu, W. Chen, Y. Huang, L. Dong and L.Wang, *ACS. Appl. Mater. Inter.,* 9 (2017) 33791-33801.
6. Y.L.Tian, X. Zhang, S.L. Dou, L.P. Zhang, H.M. Zhang, H.M. Lv, L.L.Wang, J. P. Zhao and Y. Li, *Sol. Energ. Mat. Sol. C.*, 170 (2017) 120-126.
7. S.Y. Kao, C.W. Kung, H.W. Chen, C.W. Hu and K.C.Ho, *Sol. Energ. Mat. Sol. C.* 145 (2016) 61-68.
8. S.Y.Kao, Y.S. Lin, C.W. Hu, M.K. Leung and K.C. Ho, *Sol. Energ. Mat. Sol. C.* 143 (2015) 174-182.
9. L. He, X.X. Wang and L. Duan, *ACS Appl. Mater. Inter.,* 10 (2018) 11801-11809.
10. J. Liu, J. Wu, S.Y. Shao, Y.F. Deng, B. Meng, Z.Y. Xie, Y.H. Geng, L.X. Wang and F.L. Zhang, *ACS. Appl. Mater. Inter.,*6 (2014) 8237-8245

11. H.F. Higginbotham, M. Czichy, B.K. Sharma, A.M. Shaikh, R.M. Kamble and P. Data, *Electrochim. Acta,* 273 (2018) 264-272.
12. T. Wang, T.K. Lau, X.H. Lu, J. Yuan, L.L. Feng, L.H. Jiang, W. Deng, H.J. Peng, Y.F. Li and Y.P. Zou, *Macromolecules,* 51 (2018) 2838-2846.
13. S. Xiao, Q. Zhang and W. You, *Adv. Mater.,* 29 (2017) 1601391.
14. T. Lei, J.Y.Wang and J. Pei, *Chem. Mater.,* 26 (2014) 594-603.
15. J. Mei and Z. Bao, *Chem. Mater.,* 26 (2014) 604-615.
16. H. Yao, L. Ye, H. Zhang, S. Li, S. Zhang and J. Hou, *Chem. Rev.,* 116 (2016) 7397-7457.
17. J. Yuan, Y. Zou, R. Cui, Y. H. Chao, Z. Wang, M. Ma, D. Xiao, Z. Bo, X. Xu, L. Li and C. Hsu, *Macromolecules,* 48 (2015) 4347-4356.
18. M. Abdulrazzaq, M. I. Ozkut, G. Gokce, S. Ertan, E. Tutuncu and A. Cihaner, *Electrochim. Acta,* 249 (2017) 189-197.
19. Y. B. Zhang, X. Gao, J.L. Lia and G.L. Tu, *J. Mater. Chem. C,* 3 (2015) 7463-7468.
20. J. Yuan, J. Ouyang, V. Cimrová, M. Leclerc, A. Najari and Y. Zou, *J. Mater. Chem. C.,* 5 (2017) 1858-1879.
21. M. Liu, Y. Gao, Y. Zhang, Z. Liu and L. Zhao, *Polym. Chem.,* 8 (2017) 4613-4636.
22. Y.X. Liu, M. Wang, J.S. Zhao, C.S.Cui and J.F. Liu, *RSC Adv*., 4 (2014) 52712-52726.
23. H. Zhao, D.D.Tang, J.S. Zhao, M. Wang and J.M. Dou, *RSC Adv.,* 4 (2014) 61537-61547.
24. G.R.Chagas, T. Darmanin, G. Godeau and F. Guittard, *Electrochim. Acta,* 269 (2018) 462-478.
25. B.D. Reeves, C.R.G. Grenier, A.A. Argun, A. Cirpan, T.D. McCarley and J.R. Reynolds, *Macromolecules*, 37 (2004) 7559.
26. A. Cirpan, A.A. Argun, C.R.G. Grenier, B.D. Reeves and J.R. Reynolds, *J. Mater. Chem*., 13 (2003) 2422.
27. M. Fall, L. Assogba, J.J. Aaron and M.M. Dieng, *Synthetic Met.,* 123 (2001) 365-372.
28. R. Jamal, L. Zhang, M.C.Wang, Q. Zhao and T. Abdiryim, *Prog. Nat. Sci-Mater.,* 26 (2016) 32-40.
29. J.F. Ponder, S.L. Pittelli and J.R. Reynolds, *ACS. Macro. Lett.,* 5 (2016) 714-717.
30. F.D. Feng, L.Q. Kong, H.M. Du, J.S. Zhao and J.H. Zhang, *Polymers,* 10 (2018) 427.
31. S. Chen, D. Zhang, M. Wang, L.Q. Kong and J.S. Zhao, *New J. Chem.,* 40 (2016) 2178-2188.
32. H.H. Xie, M. Wang, L.Q.Kong, Y. Zhang, X.P. Ju and J.S.Zhao, *RSC. Adv.,* 7 (2017) 11840-11851.
33. H.G. Yue, X. Guo, Y.C. Du, Y. Zhang, H.M. Du, J.S. Zhao and J.H. Zhang, *Synthetic Met*., 271(2021) 116619.
34. H. Gu, Y. Xue, F.Q. Hu, N.N. Jian, K.W. Lin, T. Wu, X.M. Liu, J.K. Xu and B.Y. Lu, *Dyes Pigments*, 183 (2020) 108648.
35. A.B. Atar, J.Y. Jeong, S.H. Han and J.S. Park, *Polymer*, 153 (2018) 95-102.
36. Q. J. Sun, H.Q.Wang, C.H.Yang and Y. F. Li, *J. Mater. Chem.,* 13 (2003) 800-806.